

# An adaptive finite element algorithm for contact problems in plasticity

P. Wriggers, O. Scherf

88

**Abstract** Due to the fact that in contact problems the contact area is not known a priori, a sufficient discretization to obtain a convergent finite element solution cannot be supplied from the outset. Therefore it is necessary to use adaptive finite element methods to adjust automatically the mesh sizes not only in the bodies under consideration but also in the contact zone. In this paper we develop an adaptive method for geometrically linear contact problems, which also includes elastoplastic material behavior. The radial return algorithm is used to derive the error estimator for one time increment of the solution process. The error estimator is based on the Zienkiewicz–Zhu projection scheme, which is extended to account for the special situation in the contact interface.

## 1

### Introduction

Contact problems in engineering are often associated with very complex geometries and nonlinear constitutive behavior. For such problems only numerical methods, like the finite element method, yield solutions of the associated mathematical model. The finite element method has been proven to be a flexible tool, especially when applied to nonlinear problems of engineering. Since numerical methods yield approximate solutions it is necessary to control the errors inherited in the method. During the last ten years research activities have been focused on adaptive techniques providing automatically a numerical model which is accurate and reliable.

In this paper we develop an adaptive method for elastoplastic contact problems which ensures successive improvement of the numerical solution via an iterative solution procedure to refine the finite element mesh. This method will be formulated for frictionless contact problems for the case of geometrically linear elastoplastic bodies.

The objective of adaptive techniques is to obtain a mesh which is optimal in the sense that the computational costs

involved are minimal under the constraint that the error in the finite element solution is beyond a certain limit. Since the computational effort can be linked to the number of unknowns of the finite element mesh the task is to find a mesh with minimum number of unknowns or nodes for a given error tolerance. In general, adaptive methods rely on error indicators and error estimators which can be computed *a priori* or *a posteriori*. For an overview over different techniques, see e.g. Johnson [5] and references therein. Based on the error distribution a new partially refined mesh can be constructed which yields a better approximate solution. To obtain an optimal mesh in the sense of an overall equal solution quality it is desirable to design the mesh such that the error contributions of the elements are equidistributed over the mesh. During the last years a growing number of papers has been devoted to this topic and applied to problems of solid and fluid mechanics, see e.g. Zienkiewicz and Taylor [25], Zienkiewicz et al. [24], Peraire et al. [15].

The methods rely on error estimators which have been developed so far in different versions. The estimators which are most frequently used in solid mechanics for elastic problems are residual based error estimators, see e.g. Babuska and Rheinboldt [2], Babuska and Miller [1], Johnson and Hansbo [7], or error estimators which use superconvergence properties, see e.g. Zienkiewicz and Zhu [26], [27]. In the case of plasticity the situation is more complex and so far no mathematically sound estimators exist for classical  $J_2$ -flow theory of plasticity. A first result has been obtained by Johnson and Hansbo [7] who developed an adaptive strategy for small strain elastoplasticity using the Hencky model. Due to the physical restrictions of the Hencky model this method cannot be applied to standard elastoplastic problems in engineering.

For  $J_2$ -flow Ortiz and Quigley [14] have developed a criterion for mesh adaption using the notion of the space of bounded variations. This criterion was successfully applied to strain localization problems. Peric et al. [16] have discussed different error estimators based on the dissipation functional, the energy norm and the rate of plastic work. The *a posteriori* error estimators rely on a post-processing concept and with this on superconvergence properties which mathematically only can be proven for meshes with a certain regularity. These estimators and the related adaption criteria have been compared by means of a strain localization problem. All developed error estimators can be applied successfully to certain classes of problems. However up to now a rigorous theoretical background is lacking.

In this contribution we will develop an error estimator for  $J_2$ -flow including contact constraints using results provided by Johnson and Hansbo [7] for the Hencky model. It will be shown

Communicated by S. N. Atluri, 18 August 1995

P. Wriggers, O. Scherf  
Institut für Mechanik, Technische Hochschule Darmstadt,  
Hochschulstr. 1, D-64289 Darmstadt, Germany

Correspondence to: P. Wriggers

The support of the Deutsche Forschungsgemeinschaft (DFG) under contract 75/604 D2 is gratefully acknowledged.

In memoriam of J. C. Simo

that the error estimator can be applied within a time increment of the solution algorithm using return mapping schemes. For frictionless contact problems *a posteriori* error estimators have been derived for linear elastic bodies, see e.g. Lee et al. [11], Wriggers et al. [23]. Here we present a new methodology to consider implicitly the physical behavior in the contact zone. This method can be applied in conjunction with smoothing procedures to compute an improved solution for the stresses.

The paper is organized as follows. First the boundary value problem for elastoplastic solids is summarized. Then we state the kinematical constraint conditions associated with contact and develop the weak formulation based on the penalty regularization. A summary of the basic return mapping algorithms for elastoplasticity provides the basis for a reformulation of the incremental equations for the error estimation. After the spatial discretization using finite elements the error estimators for contact and elastoplasticity are presented. Finally an algorithm for the adaptive method is developed which relies on the derived error estimates applied to the incremental nonlinear problem. The  $h$ -adaptive algorithm is applied to a test example.

## 2

### Formulation of the elastoplastic continuum problem

Let us recall the basic equations of an elastoplastic solid for the case of metal plasticity undergoing small strains. We denote by  $\boldsymbol{\varepsilon}$  the total strains which are decomposed additively into an elastic,  $\boldsymbol{\varepsilon}^e$ , and a plastic part  $\boldsymbol{\varepsilon}^p$  as follows

$$\boldsymbol{\varepsilon}(\mathbf{u}) = \boldsymbol{\varepsilon}^e(\mathbf{u}) + \boldsymbol{\varepsilon}^p(\mathbf{u}) \quad \text{with} \quad \boldsymbol{\varepsilon}(\mathbf{u}) = \frac{1}{2}(\text{Grad } \mathbf{u} + \text{Grad}^T \mathbf{u}). \quad (1)$$

Local equilibrium yields

$$\text{div } \boldsymbol{\sigma} + \hat{\mathbf{b}} = \mathbf{0}, \quad (2)$$

with given body forces  $\hat{\mathbf{b}}$ . The standard boundary conditions are

$$\mathbf{u} = \mathbf{0} \quad \text{on } \Gamma_u \quad \text{and} \quad \boldsymbol{\sigma} \mathbf{n} = \hat{\mathbf{t}} \quad \text{on } \Gamma_\sigma, \quad (3)$$

where  $\mathbf{n}$  denotes the outward unit normal vector on  $\Gamma$  and  $\hat{\mathbf{t}}$  are applied boundary loads.

Equations (1) to (3), characterizing the displacements  $\mathbf{u}$ , are equivalent to the following weak formulation: Find  $\mathbf{u} \in \mathcal{V}$  such that

$$\int_{\Omega} [\boldsymbol{\sigma}(\mathbf{u}) : \boldsymbol{\varepsilon}(\mathbf{v}) - \hat{\mathbf{b}} \cdot \mathbf{v}] d\Omega - \int_{\Gamma_\sigma} \hat{\mathbf{t}} \cdot \mathbf{v} d\Gamma = 0 \quad \forall \mathbf{v}, \quad (4)$$

where  $\mathbf{v}$  denotes the virtual displacement or test function.

Furthermore we can summarize the constitutive equations for an elastoplastic solid with linear isotropic hardening. The stresses  $\boldsymbol{\sigma}$  and the hardening variable  $q$  can be obtained for a homogeneous material from a free energy function  $\Psi(\boldsymbol{\varepsilon}^e, \alpha)$  according to

$$\boldsymbol{\sigma} = \frac{\partial \Psi}{\partial \boldsymbol{\varepsilon}^e} \quad \text{and} \quad q = -\frac{\partial \Psi}{\partial \alpha}. \quad (5)$$

Since we restrict ourselves to classical plasticity and linear hardening the free energy function is given by

$$\Psi(\boldsymbol{\varepsilon}^e, \alpha) = \frac{1}{2} \boldsymbol{\varepsilon}^e : \mathbf{C} : \boldsymbol{\varepsilon}^e + \frac{1}{2} K \alpha^2, \quad (6)$$

where  $\mathbf{C}$  is the elasticity tensor and  $K$  denotes the hardening modulus. This leads with (5) to the following constitutive relations

$$\boldsymbol{\sigma} = \mathbf{C} : (\boldsymbol{\varepsilon} - \boldsymbol{\varepsilon}^p) \quad \text{and} \quad q = -K \alpha. \quad (7)$$

The elastic region is determined from the yield condition

$$f(\boldsymbol{\sigma}, \alpha) = |\mathbf{s}| - \sqrt{\frac{2}{3}} (Y_0 + K \alpha) \leq 0. \quad (8)$$

Here  $\mathbf{s} = \boldsymbol{\sigma} - \frac{1}{3} \text{tr } \boldsymbol{\sigma} \mathbf{1}$  denotes the deviatoric stress and  $Y_0$  is the initial yield stress. The flow rule and hardening law are given for associated plastic flow by

$$\dot{\boldsymbol{\varepsilon}}^p = \gamma \frac{\partial f}{\partial \boldsymbol{\sigma}} = \gamma \frac{\mathbf{s}}{|\mathbf{s}|} \quad \text{and} \quad \dot{\alpha} = \gamma \frac{\partial f}{\partial q} = \gamma \sqrt{\frac{2}{3}}. \quad (9)$$

The loading, respectively unloading, conditions can be stated in Kuhn-Tucker form

$$\gamma \geq 0, \quad f(\boldsymbol{\sigma}, \alpha) \leq 0 \quad \text{and} \quad \gamma f(\boldsymbol{\sigma}, \alpha) = 0, \quad (10)$$

which completes the elastoplastic model together with the consistency condition

$$\gamma \dot{f}(\boldsymbol{\sigma}, \alpha) = 0. \quad (11)$$

## 3

### Formulation of the contact problem

Let us consider two bodies  $\mathcal{B}^\alpha$ ,  $\alpha = 1, 2$ , each of them occupying the bounded domain  $\Omega^\alpha \subset \mathbb{R}^2$ . The boundary  $\Gamma^\alpha$  of a body  $\mathcal{B}^\alpha$  can in general be splitted into three parts:  $\Gamma^\alpha_u$  with prescribed surface loads,  $\Gamma^\alpha_v$  with prescribed displacements and  $\Gamma^\alpha_c$  where the two bodies  $\mathcal{B}^1$  and  $\mathcal{B}^2$  come into contact. Next the contact conditions, the weak form of the associated problem and the penalty regularization of the contact constraints will be stated.

### 3.1

#### Contact kinematics

Assume that two bodies come into contact. In that case we have to find the minimum distance of a point on the surface of one body with respect to the other one. The associated mathematical formulation for this case can be found in e.g. Laursen and Simo [10], Wriggers and Miehe [22]. It yields the non-penetration condition in terms of the coordinates  $\mathbf{x}^\alpha = \mathbf{X}^\alpha + \mathbf{u}^\alpha$  of the current configuration of the bodies  $\mathcal{B}^\alpha$

$$[\mathbf{x}^1 - \hat{\mathbf{x}}^2(\bar{\boldsymbol{\xi}})] \cdot \mathbf{n}_c \geq 0. \quad (12)$$

Here  $\bar{\boldsymbol{\xi}}$  denote the surface coordinates of body  $\mathcal{B}^2$  and  $\mathbf{n}_c$  the surface normal on  $\Gamma_c^2$  with respect to the current configuration. The point  $\hat{\mathbf{x}}^2(\bar{\boldsymbol{\xi}})$  is found from the minimal distance problem

which associates to every point  $\mathbf{x}^1$  on  $\Gamma_c^1$  a point  $\hat{\mathbf{x}}^2(\bar{\xi})$  on  $\Gamma_c^2$  via

$$\|\mathbf{x}^1 - \hat{\mathbf{x}}^2(\bar{\xi})\| = \min_{\mathbf{x}^2 \in \Gamma_c^2} \|\mathbf{x}^1 - \mathbf{x}^2\|, \quad (13)$$

see e.g. Wriggers and Miehe [22]. Since we restrict ourselves in this paper to the case of small deformations we can use the displacement field instead of the deformation itself. The associated linearization then leads to the non-penetration condition

$$(\mathbf{u}^1 - \hat{\mathbf{u}}^2) \cdot \mathbf{n}_c + g \geq 0, \quad (14)$$

where the initial gap  $g$  between the two bodies is given by  $g = (\mathbf{X}^1 - \hat{\mathbf{X}}^2) \cdot \mathbf{n}_c$ .  $\mathbf{n}_c$  is the surface normal with respect to the reference configuration on  $\Gamma_c^2$ .

In view of the penalty formulation which will be applied to solve the contact problems we introduce a penetration function as follows:

$$u_n^- = \begin{cases} (\mathbf{u}^1 - \hat{\mathbf{u}}^2) \cdot \mathbf{n}_c + g & \text{if } (\mathbf{u}^1 - \hat{\mathbf{u}}^2) \cdot \mathbf{n}_c + g < 0 \\ 0 & \text{otherwise.} \end{cases} \quad (15)$$

Function (15) indicates the penetration of one body into the other and shows in which parts of  $\Gamma^*$  the constraint equations preventing penetration have to be activated. Thus (15) can be used to determine the contact area.

**Remark** In the case of contact between a rigid surface and a deformable body the above equations also hold. Then we set  $\hat{\mathbf{u}}^2 \equiv \mathbf{0}$  and  $\mathbf{n}_c$  represents the normal of the rigid surface.

### 3.2

#### The weak form of the boundary value problem with contact

In the previous section we distinguished between the deformations  $\mathbf{x}^\alpha$  to define the penetration function. This is no longer necessary since the subsequent equations are valid for every point  $X \in \mathcal{B}^\alpha$ . Therefore we omit the index  $\alpha$  in the following for convenience knowing that in case of different constitutive equations for  $\mathcal{B}^1$  and  $\mathcal{B}^2$  we have to make a distinction.

If contact constraints are present, the weak formulation (4) can be recast as follows:

$$\int_{\Omega} \boldsymbol{\sigma}(\mathbf{u}) : \boldsymbol{\varepsilon}(\mathbf{v} - \mathbf{u}) d\Omega \geq \int_{\Omega} \hat{\mathbf{b}} \cdot (\mathbf{v} - \mathbf{u}) d\Omega + \int_{\Gamma_c} \hat{\mathbf{t}} \cdot (\mathbf{v} - \mathbf{u}) d\Gamma \quad (16)$$

and  $\Omega \equiv \bigcup_{\alpha} \Omega^\alpha$ ,  $\Gamma_\sigma = \bigcup_{\alpha} \Gamma_\sigma^\alpha$ . The contact problem is now to find  $\mathbf{u} \in \mathcal{K}$  such that (16) is fulfilled for all  $\mathbf{v} \in \mathcal{K}$  with

$$\mathcal{K} = \{ \mathbf{v} \in \mathcal{V} \mid (\mathbf{v}^1 - \hat{\mathbf{v}}^2) \cdot \mathbf{n}_c + g \geq 0 \text{ on } \Gamma_c \} \quad (17)$$

Due to the inequality constraint on the displacement field this problem is nonlinear even for the linear elastic case.

Here the solution of the contact problem is obtained using the penalty method, see e.g. Luenberger [12]. This technique replaces the variational inequality by an unconstrained problem with regard to the contact constraint (14) as follows: Find  $\mathbf{u} \in \mathcal{V}$  such that

$$\int_{\Omega} \boldsymbol{\sigma}(\mathbf{u}) : \boldsymbol{\varepsilon}(\mathbf{v}) d\Omega + \int_{\Gamma_c^1} \varepsilon u_n^- \nu_n d\Gamma = \int_{\Omega} \hat{\mathbf{b}} \cdot \mathbf{v} d\Omega + \int_{\Gamma_c} \hat{\mathbf{t}} \cdot \mathbf{v} d\Gamma \quad \forall \mathbf{v} \in \mathcal{V}. \quad (18)$$

$u_n^-$  has already been defined in (15) and  $\nu_n = (\mathbf{v}^1 - \hat{\mathbf{v}}^2) \cdot \mathbf{n}_c$ . The penalty parameter  $\varepsilon$  is a positive constant. For linear elasticity it can be shown, see e.g. Kikuchi and Oden [8] or Carstensen et al. [3], that the solution of the regularized problem will converge to the solution of the original contact problem as  $\varepsilon$  tends to infinity.

### 4

#### Return mapping algorithm for elasto-plasticity

For the solution of an elastoplastic problem we have to integrate the evolution Eqs. (7) to (10) governing the plastic flow. For this purpose the so called return mapping algorithms are applied, which have been established during the last years and represent now the standard tool for the solution of elastoplastic problems, see e.g. the overview article by Simo [18].

The solution of the elastoplastic evolution equations leads to an incremental problem in which a time discretization of the interesting time interval  $\{t_0, t_1, \dots, t_n, t_{n+1}, \dots, t_e\}$  is used. Within a time step  $[t_n, t_{n+1}]$  we have the internal variables  $\boldsymbol{\varepsilon}_n^p$  and  $\alpha_n$  as initial data. Furthermore we assume that the displacement field  $\mathbf{u}_{n+1}$  and thus the strains  $\boldsymbol{\varepsilon}(\mathbf{u}_{n+1})$  are known which e.g. has been computed by the spatial finite element method. Since the return mapping algorithms are very well established we like to state here only the resulting equations which have been used for our own computations and which will be needed subsequently for the error estimation. For a concise treatment of these algorithms, see Simo [18].

We use the standard implicit backward Euler algorithm for Eqs. (1), (7) to (10) which yields the following algorithm:

- Compute a 'trial' state

$$\mathbf{s}_{n+1}^{tr} = 2\mu(\mathbf{e}_{n+1} - \mathbf{e}_n^p) \quad (19)$$

$$\alpha_{n+1}^{tr} = \alpha_n \quad (20)$$

- Perform the return map

$$\mathbf{s}_{n+1} = \mathbf{s}_{n+1}^{tr} - 2\mu\Delta\gamma \mathbf{n}_{n+1} \quad (21)$$

$$\alpha_{n+1} = \alpha_{n+1}^{tr} + \sqrt{\frac{2}{3}} \Delta\gamma, \quad (22)$$

where the definitions for the deviators

$$\mathbf{s}_{n+1} = \boldsymbol{\sigma}_{n+1} - \frac{1}{3} \text{tr} \boldsymbol{\sigma}_{n+1} \mathbf{1} \quad \text{and} \quad \mathbf{e}_{n+1} = \boldsymbol{\varepsilon}_{n+1} - \frac{1}{3} \text{tr} \boldsymbol{\varepsilon}_{n+1} \mathbf{1} \quad (23)$$

and the normal to the yield surface

$$\mathbf{n}_{n+1} = \frac{\mathbf{s}_{n+1}^{tr}}{|\mathbf{s}_{n+1}^{tr}|} = \frac{\mathbf{s}_{n+1}}{|\mathbf{s}_{n+1}|} \quad (24)$$

have been used. For linear isotropic hardening the consistency parameter  $\Delta\gamma$  can be stated in closed form

$$\Delta\gamma = \frac{f_{n+1}^{tr}}{2\mu + \frac{2}{3}K} \quad \text{with} \quad f_{n+1}^{tr} = |\mathbf{s}_{n+1}^{tr}| - \sqrt{\frac{2}{3}}(Y_0 + K \alpha_{n+1}^{tr}). \quad (25)$$

This completes the update of the deviatoric elastoplastic stresses  $\mathbf{s}_{n+1}$  and the hardening variable  $\alpha_{n+1}$  within one time step. This local update has to be included in a global Newton iteration for the solution of the boundary value problem at hand.

For later use we will now solve Eqs. (19) to (25) for the total deviatoric strain  $\mathbf{e}_{n+1}$ . After some algebra we arrive at

$$\mathbf{e}_{n+1} - \mathbf{e}_n^p = \frac{1}{2\mu} \mathbf{s}_{n+1} + \frac{3}{2K} \left( \mathbf{s}_{n+1} - \frac{\sqrt{\frac{2}{3}}(Y_0 + K\alpha_n)}{|\mathbf{s}_{n+1}|} \mathbf{s}_{n+1} \right). \quad (26)$$

Noting that the yield condition is at time  $t_n$  given by

$$f_n = |\mathbf{s}_n| - \sqrt{\frac{2}{3}}(Y_0 + K\alpha_n) \leq 0 \quad (27)$$

we can define an incremental projection operator  $\Pi(\mathbf{s}_{n+1})$  in an analogous way as in Johnson and Hansbo [7].

$$\Pi(\mathbf{s}_{n+1}) = \begin{cases} \mathbf{s}_{n+1} & \text{for elastic loading} \\ \frac{|\mathbf{s}_n|}{|\mathbf{s}_{n+1}|} \mathbf{s}_{n+1} & \text{for plastic loading} \end{cases} \quad (28)$$

and obtain for the strain deviator  $\mathbf{e}_{n+1}$

$$\mathbf{e}_{n+1} - \mathbf{e}_n^p = \frac{1}{2\mu} \mathbf{s}_{n+1} + \frac{3}{2K} (\mathbf{s}_{n+1} - \Pi(\mathbf{s}_{n+1})). \quad (29)$$

To arrive at an expression for the total strain  $\boldsymbol{\varepsilon}_{n+1}$  we have to add in (29) the elastic volumetric strains which then leads to

$$\boldsymbol{\varepsilon}_{n+1} - \mathbf{e}_n^p = \frac{1}{2\mu} \mathbf{s}_{n+1} + \frac{1}{9\hat{K}} \text{tr} \boldsymbol{\sigma}_{n+1} \mathbf{1} + \frac{3}{2K} [\mathbf{s}_{n+1} - \Pi(\mathbf{s}_{n+1})], \quad (30)$$

where  $\hat{K}$  denotes the bulk modulus.

Note that Eq. (30) is valid within a time increment  $[t_n, t_{n+1}]$  and  $\mathbf{e}_n^p$  is an initial data. So far we have only performed a discretization in time and not assumed that the field variables result from an approximate solution, e.g. by using the finite element discretization.

## 5 Spatial discretization by finite elements

To discretize the linear elastoplastic contact problem defined above we divide the domain  $\Omega$  occupied by the bodies  $\mathcal{B}^z$  into non-overlapping finite elements  $T$  of diameter  $h_T$  and introduce a standard finite element space

$$\mathcal{V}_h = \{ \mathbf{v} \in \mathcal{V} \mid \mathbf{v} \in C(\Omega), \mathbf{v}|_T \in [\mathcal{P}(T)]^2 \forall T \}, \quad (31)$$

where  $\mathcal{P}(T)$  is a space of polynomials of degree  $p_T$  on  $T$  and  $p_T$  is a positive integer. Moreover the boundary is assumed to be piecewise affine such that the triangulation covers  $\Omega$  exactly and the type of boundary condition does not change on a side of an element. The discrete finite element problem yields now in the time increment  $[t_n, t_{n+1}]$ : Find  $\mathbf{u}_{h,n+1} \in \mathcal{V}_h$  such that

$$\begin{aligned} G(\mathbf{u}_{h,n+1}) &= \int_{\Omega} \boldsymbol{\sigma}(\mathbf{u}_{h,n+1}) : \boldsymbol{\varepsilon}(\mathbf{v}_h) d\Omega - \int_{\Omega} \hat{\mathbf{b}} \cdot \mathbf{v}_h d\Omega - \int_{\Gamma_r} \hat{\mathbf{t}} \cdot \mathbf{v}_h d\Gamma \\ &\quad - \int_{\Gamma_c^+} \boldsymbol{\varepsilon}(\mathbf{u}_{h,n+1})_n^-(\mathbf{v}_h)_n d\Gamma = 0 \quad \forall \mathbf{v}_h \in \mathcal{V}_h. \end{aligned} \quad (32)$$

To solve this nonlinear equation within the time step Newton's method is applied which leads to the following

iterative scheme for the displacement field at time  $t_{n+1}$ :

$$DG(\mathbf{u}_{h,n+1}^i)|_{\mathbf{u}_{h,n+1}^i} \Delta \mathbf{u}_h^{i+1} = -G(\mathbf{u}_{h,n+1}^i), \quad \mathbf{u}_{h,n+1}^{i+1} = \mathbf{u}_{h,n+1}^i + \Delta \mathbf{u}_h^{i+1}, \quad (33)$$

with the starting value:  $\mathbf{u}_{h,n+1}^0 = \mathbf{u}_{h,n}$ . The operator  $D$  denotes the tangent matrix of  $G$  which can be obtained for elastoplastic problems with the aid of the derivation given in the classical paper by Simo and Taylor (1985). Since the contact kinematics are assumed to be linear, see (14), the nonlinearity associated with the contact is only due to the changing number of contact constraints within the iteration.

## 6

### Error estimator for contact and elastoplasticity

In this section we will present an error estimator which can be used for elastoplastic contact problems. This estimate relies on smoothing procedures in the sense of the Zienkiewicz and Zhu [26] error estimators and can be applied to  $J_2$ -flow theory.

Let  $\mathbf{u}_{n+1}$  denote the exact solution of (18) for the given time discretization by the return mapping schemes, see Sect. 4 and let  $\mathbf{u}_{h,n+1}$  denote the discrete FEM-solution of (32). To simplify notation and for convenience we will omit the index  $n+1$  in the following derivations, thus  $\mathbf{u}_{n+1} \rightarrow \mathbf{u}$  and  $\mathbf{u}_{h,n+1} \rightarrow \mathbf{u}_h$ . With

$$\hat{\mathbf{e}} = \mathbf{u} - \mathbf{u}_h \quad (34)$$

we define the error in the displacement field within the time step under consideration.

To derive an error estimator we subtract the finite element approximation of (30) from (30) leading to

$$\begin{aligned} (\boldsymbol{\varepsilon} - \mathbf{e}_n^p) - (\boldsymbol{\varepsilon}_h - \mathbf{e}_{h,n}^p) &= \frac{1}{2\mu} (\mathbf{s} - \mathbf{s}_h) + \frac{1}{9\hat{K}} \text{tr}(\boldsymbol{\sigma} - \boldsymbol{\sigma}_h) \mathbf{1} \\ &\quad + \frac{3}{2K} [\mathbf{s} - \Pi(\mathbf{s}) - (\mathbf{s}_h - \Pi(\mathbf{s}_h))]. \end{aligned} \quad (35)$$

The multiplication of this equation by  $(\boldsymbol{\sigma} - \boldsymbol{\sigma}_h)$  and its integration over the domain  $\Omega$  yields

$$\| \boldsymbol{\sigma} - \boldsymbol{\sigma}_h \|_{E^{-1}}^2 \leq \int_{\Omega} [ \boldsymbol{\varepsilon}(\hat{\mathbf{e}}) - (\mathbf{e}_n^p - \mathbf{e}_{h,n}^p) ] : (\boldsymbol{\sigma} - \boldsymbol{\sigma}_h) d\Omega \quad (36)$$

In this step we have further used that  $[\mathbf{s} - \Pi(\mathbf{s}) - (\mathbf{s}_h - \Pi(\mathbf{s}_h))] : (\mathbf{s} - \mathbf{s}_h) \geq 0$ , a result obtained by Johnson and Hansbo [7].

$\|\cdot\|_{E^{-1}}$  denotes the complementary energy norm, defined by

$$\| \boldsymbol{\sigma} \|_{E^{-1}}^2 = \int_{\Omega} \left[ \frac{1}{2\mu} \mathbf{s} : \mathbf{s} + \frac{1}{9\hat{K}} (\text{tr} \boldsymbol{\sigma})^2 \right] d\Omega. \quad (37)$$

The equivalence of this norm to the energy norm can be shown easily by inserting the constitutive equations for elasticity into the last expression leading to  $\| \boldsymbol{\sigma} - \boldsymbol{\sigma}_h \|_{E^{-1}}^2 = \| \hat{\mathbf{e}} \|_E^2$ .

Equation (36) is almost equal to that reported in Johnson and Hansbo [7] for the Hencky model. The only difference is the appearance of the initial data, the exact,  $\mathbf{e}_n^p$ , and the approximated,  $\mathbf{e}_{h,n}^p$ , plastic strains at time  $t_n$ .

A possibility to derive an error estimator for elastoplasticity is provided by a reformulation of Eq. (36). We observe that the total strain can be split into an elastic and a plastic part which yields

$$\boldsymbol{\varepsilon}_{n+1} = \boldsymbol{\varepsilon}_{n-1}^e + \boldsymbol{\varepsilon}_{n+1}^p \rightarrow \boldsymbol{\varepsilon}_{n-1} - \boldsymbol{e}_n^p = \boldsymbol{\varepsilon}_{n+1}^e + \Delta \boldsymbol{e}_{n-1}^p, \quad (38)$$

where we have defined the increment of the plastic deformation as the difference  $\Delta \boldsymbol{e}_{n+1}^p = \boldsymbol{e}_{n+1}^p - \boldsymbol{e}_n^p$ . Thus Eq. (36) leads to

$$\|\boldsymbol{\sigma} - \boldsymbol{\sigma}_h\|_{L^2}^2 \leq \int_{\Omega} [(\Delta \boldsymbol{e}^p - \Delta \boldsymbol{e}_h^p) : (\boldsymbol{\sigma} - \boldsymbol{\sigma}_h) + (\boldsymbol{\varepsilon}^e - \boldsymbol{\varepsilon}_h^e) : (\boldsymbol{\sigma} - \boldsymbol{\sigma}_h)] d\Omega. \quad (39)$$

This equation can be interpreted as follows. The first term denotes the error due to the plastic dissipation within the time increment whereas the second term is related to the elastic response in the plastic zone. Both terms can now be approximated by using smoothing procedures leading to  $Z^2$ -type error measures. Note that  $\boldsymbol{\varepsilon}^e$  is not in general a gradient of the ‘elastic’ displacement field. Thus the development of a residual error estimator is not possible in the standard way. With the projections

$$\begin{aligned} \mathbb{P}[\boldsymbol{\varepsilon}^e - \boldsymbol{\varepsilon}(\mathbf{u}_h)^e] &= \mathbf{0}, \\ \mathbb{P}[\Delta \boldsymbol{e}^p - \Delta \boldsymbol{e}_h^p] &= \mathbf{0}, \\ \mathbb{P}[\boldsymbol{\sigma} - \boldsymbol{\sigma}_h] &= \mathbf{0}, \end{aligned} \quad (40)$$

which can be a  $L^2$ -projection or a discrete projection scheme, e.g. basing on superconvergent properties of the finite elements, we obtain the final result

$$\|\boldsymbol{\sigma} - \boldsymbol{\sigma}_h\|_{L^2}^2 \leq \int_{\Omega} [(\Delta \boldsymbol{e}^p - \Delta \boldsymbol{e}_h^p) : (\boldsymbol{\sigma} - \boldsymbol{\sigma}_h) + (\boldsymbol{\varepsilon}^e - \boldsymbol{\varepsilon}_h^e) : (\boldsymbol{\sigma} - \boldsymbol{\sigma}_h)] d\Omega. \quad (41)$$

Note that the error estimator (41) is in accordance with the error estimator proposed by Peric et al. [16] who introduced an error measure of the plastic dissipation on a more *ad hoc* basis for problems with strain localization which we have so far excluded in our formulation.

This error estimate has been developed for one time step within the numerical simulations of an elastoplastic flow problem. So far we did not address the error inherited in the time integration procedure. This would be the next step which will then allow the adjustment of the time increments. Results concerning the accuracy and convergence properties of different return mapping schemes can be found in e.g. Krieg and Krieg [9], Ortiz and Popov [13], Simo [17] or [18].

The error estimator (41) does not include special boundary terms for the contact contributions. The estimate for the contact area is in this case included implicitly since the integral in (41) has to be evaluated with respect to  $\Omega = \bigcup_x \Omega^e$  and thus includes also the contact interface.

To compute  $\boldsymbol{\varepsilon}^e$ ,  $\Delta \boldsymbol{e}^p$  and  $\boldsymbol{\sigma}$ , we apply the superconvergent patch recovery technique, proposed by Zienkiewicz and Zhu [27]. This technique uses points within a finite element,

where the quantities related to the gradient of the solution, e.g. strains and stresses, exhibit a higher order of convergence. From these sampling points the stresses and strains are projected locally onto a node by using an element patch, which consists of all elements connected with the node considered.

A polynomial expansion of the function describing the derivatives is then fitted in a least square sense to the sampling point values within the patch. For the expansion the same polynomial degree as for the basis functions is chosen, with the object to preserve the higher convergence rate. In a next step the nodal values are calculated by inserting the nodal coordinates into the polynomial expansion. Finally, the improved solution is interpolated globally with the recovered nodal values and the standard basis functions, which are also used for the interpolation of the displacements. For a detailed description of the methodology we refer to Zienkiewicz and Zhu [27].

Since we are concerned here with frictionless contact, we can assume a principle stress state in the contact zone. According to local equilibrium the normal stress must be equal in adjacent points on  $\Gamma_c^1$  and  $\Gamma_c^2$ . This physical information can be used during stress smoothing to consider implicitly the presence of contact. For that purpose we search the closest located node  $I$  on  $\Gamma_c^2$  to a node  $K$  on  $\Gamma_c^1$ , see Fig. 1. All elements, which are connected with node  $I$ , determine the extended patch, while all elements connected with  $K$  define the standard patch. Next, we compute in the Gaussian points of all patch elements the principal stresses. As a consequence of the contact physics we can now use for the projection of the normal stress the sampling points in the standard and in the extended patch. Concerning the stress tangential to  $\Gamma_c$ , we have to take in general different stress states on  $\Gamma_c^1$  and  $\Gamma_c^2$  into account. Thus only elements connected with  $K$  can be considered for the projection of the tangential stresses. The recovered principal stresses must then be transformed to global coordinates, since on nodes, which are not contained in  $\Gamma_c^2$ , the stress tensor coefficients are projected directly. Therefore we need the principal axes in  $K$ , which are associated with the normal vector, given by

$$\mathbf{n}_{cK} = \begin{bmatrix} n_x \\ n_y \end{bmatrix} = \frac{1}{2} (\mathbf{n}_c^r + \mathbf{n}_c^l), \quad (42)$$

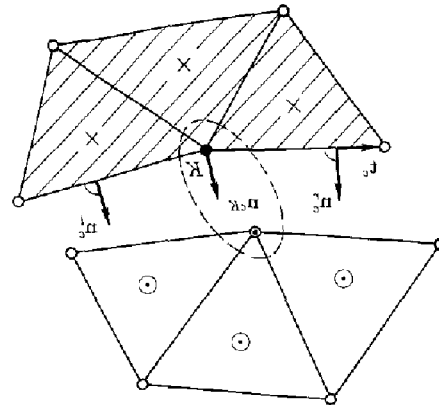


Fig. 1. Element patch, contact interface  $\odot$  Gaussian point, extended patch  $\times$  Gaussian point, standard patch

see Fig. 1. The transformation is then performed in a standard way:

$$\bar{\sigma}_{K,\text{glob}}^* = \mathbf{N} \bar{\sigma}_{K,\text{prim}}^* \mathbf{N}^T, \quad \mathbf{N} = \begin{bmatrix} n_y & n_x \\ -n_x & n_y \end{bmatrix}. \quad (43)$$

## 7 Adaptive mesh refinement

The adaptive refinement strategy for the elastoplastic contact problem is developed in this section. For this purpose we first state the refinement criterion which is based on the considerations of the previous sections. After that we shortly discuss our implementation for the transfer of field and history variables. Finally the overall solution algorithm is introduced. For further reference we would like to summarize the error estimator developed in the last section:

$$E_T^2 = \int_T [(\Delta \mathbf{e}^p - \Delta \mathbf{e}_h^p) : (\bar{\sigma}^* - \sigma_h) + (\bar{\varepsilon}^e - \varepsilon_h^e) : (\bar{\sigma}^* - \sigma_h)] d\Omega. \quad (44)$$

### 7.1 Refinement strategy

The object of an adaptive algorithm is usually stated as a nonlinear optimization problem: construct a mesh such that the associated FEM-solution satisfies

$$\|\sigma - \sigma_h\|_{E^-} = \|\mathbf{u} - \mathbf{u}_h\|_E \leq \sqrt{\sum_T E_T^2} \leq \text{TOL}, \quad (45)$$

with  $\text{TOL}$  being a given tolerance. Furthermore the expense to compute  $\mathbf{u}_h$  or  $\sigma_h$  should be nearly minimal. As a measure of computational work the total number of degrees of freedom is chosen. Since the exact solution  $\mathbf{u}$  is not known we demand that the sum of the error contributions of all elements yields

$$\sum_T E_T^2 \leq \text{TOL}^2, \quad (46)$$

which guarantees that (45) is fulfilled. (46) serves as a stopping criterion in the adaptive process. To minimize the number of degrees of freedom during refinement, we require that the mesh is an optimal mesh, i.e. that the error  $E_T^2$  is equally distributed between elements:

$$\sum_T E_T^2 = N \bar{E}_T^2. \quad (47)$$

$N$  denotes the number of elements in the mesh. Finally (47) yields together with (46) the refinement criterion

$$E_T^2 \leq \frac{\text{TOL}^2}{N}. \quad (48)$$

### 7.2 Transfer of field and history variables

An incremental solution procedure in conjunction with mesh refinement and mesh smoothing requires a general projection scheme for various field variables from a mesh  $\mathcal{F}^i$  to a mesh  $\mathcal{F}^{i+1}$ .

For the displacement field transfer we use the standard interpolation

$$\mathbf{u}_J^{i+1} = \sum_I N_I(\mathbf{x}_J) \mathbf{u}_I^i, \quad (49)$$

where  $\mathbf{x}_J$  denote the coordinates and  $\mathbf{u}_J^{i+1}$  the displacements of node  $J$  in  $\mathcal{F}^{i+1}$ . The nodes  $I$  in  $\mathcal{F}^i$  belong to an element  $T \in \mathcal{F}^i$ , which contains node  $J$ .  $N_I$  are the basis functions connected with nodes  $I$ .

The field of history variables is projected in a similar manner. Since the history variables are computed at the Gaussian points we use a 'virtual' triangular mesh  $\mathcal{M}^i$ , defined by the Gaussian points of  $\mathcal{F}^i$ . Further we search for the element  $M \in \mathcal{M}^i$  which contains a Gaussian point  $G_i^{j+1}$  of an element  $T \in \mathcal{F}^{i+1}$ .  $M$  is defined by its virtual nodes  $G_i^j$ . If  $G_i^{j+1}$  is not contained in  $\mathcal{M}^i$ , a case which can appear if  $G_i^{j+1}$  is situated near the boundary of  $\mathcal{F}^i$ , the element  $M$  located closest to  $G_i^{j+1}$  is used. Then the interpolation is performed as follows:

$$\mathbf{h}_J^{i+1} = \sum_I N_I(\mathbf{x}_J) \mathbf{h}_I^i, \quad (50)$$

with  $\mathbf{h}_J^{i+1}$  as the history variables at point  $G_i^{j+1}$ .  $\mathbf{x}_J$  denote the coordinates of  $G_i^{j+1}$  and  $\mathbf{h}_I^i$  are the history variables at point  $G_i^i$ . The basis functions  $N_I$  are associated with  $G_i^i$  and extended outwards the area of  $M$  if  $G_i^{j+1} \notin \mathcal{M}^i$ .

### 7.3 Solution algorithm

Now we state the overall algorithm of our  $h$ -adaptive method for contact problems in plasticity. The algorithm includes the following steps:

1. Set initial values:  $l = 0$ ,  $\lambda_0 = 0$ ,  $\Delta\lambda$ ,  $i = 0$
2. Generation of start mesh:  $\mathcal{F}_i$
3. Loop over load increments:  $\lambda_{i+1} = \lambda_i + \Delta\lambda$ 
  - 3.1 IF  $\lambda_{i+1} > \lambda_{\text{max}} \Rightarrow \text{STOP}$
  - 3.2 Iteration loop to solve nonlinear problem
  - 3.3 Mesh optimization
    - Compute  $E_T^2$
    - IF  $\sum E_T^2 < \text{TOL}^2 \Rightarrow \text{GO TO 3}$ .
    - IF  $E_T^2 > \text{TOL}^2/N \Rightarrow \text{refine element T}$
    - Set  $i = i + 1$
    - Generate new mesh  $\mathcal{F}_{i+1}$   
Delaunay triangularization  
Smoothing
    - Interpolate displacement and history variables on the new mesh
    - GO TO 3.2

## 8 Numerical example

The introduced adaptive algorithm has been implemented in the Finite Element Analysis Program (FEAP), developed by R. L. Taylor, see [25]. The mesh is defined via a parametric surface description of the boundaries. All loads, boundary constraints and contact constraints are defined with respect to these surfaces. A Delaunay triangularization is then used to create the successive meshes during the adaptive process; for the associated algorithm, see Sloan [21]. Throughout the computations we apply linear triangular elements.

We consider now a problem, where an elastic sphere (Young's modulus  $E = 2.1 \cdot 10^7$ , Poisson's ratio  $\nu = 0.3$ ) comes into contact with a beam, see Fig. 2 for the initial mesh. The material of the beam is elastoplastic ( $E = 2.1 \cdot 10^5$ ,  $\nu = 0.3$ ,  $Y_0 = 500$ ,  $K = 5000$ ). Plane strain conditions are assumed. The geometry of the problem is defined by the following data: Length of the beam  $l = 4$ , height of the beam  $h = 1$ , radius of the sphere  $r = 1$ . Both ends of the beam are clamped and at the upper boundary of the sphere a uniform pressure is applied. This load is increased linearly to a final value of 175 with 7 time steps of  $\Delta t = 0.5$ . Due to the symmetry of the problem, only half of the structure is discretised. The tolerance for the adaptive algorithm is given by  $TOL = 0.1$ .

In a sequence of pictures, Figs. 2 to 15, we show the development of the plastic zone in combination with the values of the error indicators and adaptive mesh refinement.

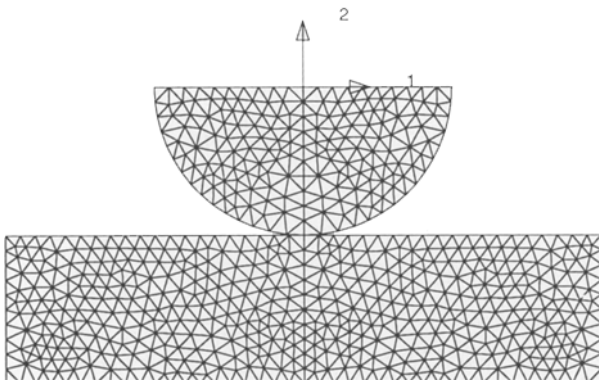


Fig. 2. First mesh, 353 nodes, 607 elements

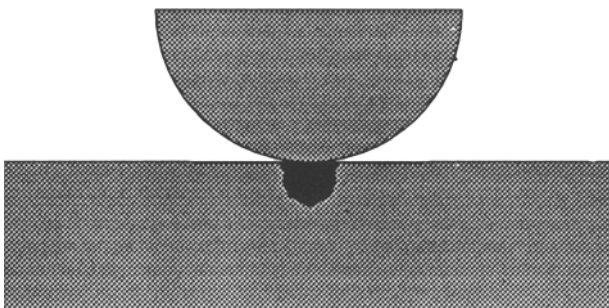


Fig. 3. First mesh, plastic zone,  $t = 1.5$

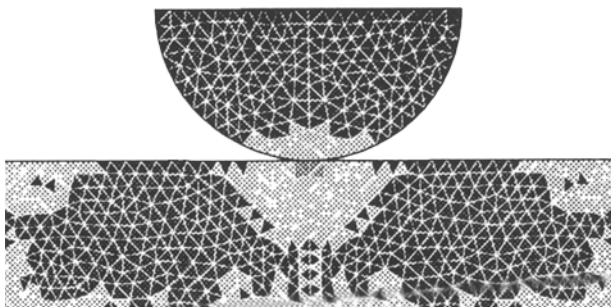


Fig. 4. First mesh, error distribution

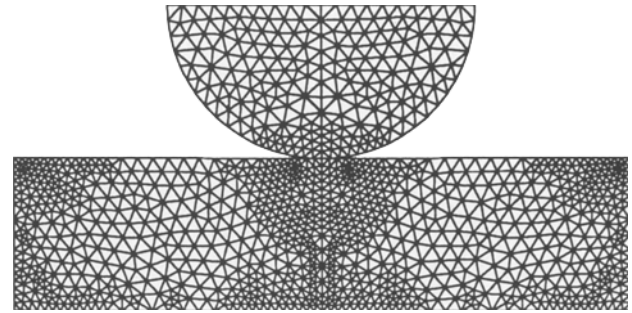


Fig. 5. Second mesh, 633 nodes, 1126 elements

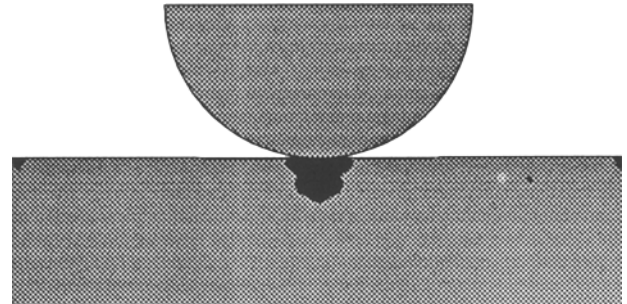


Fig. 6. Second mesh, plastic zone,  $t = 1.5$

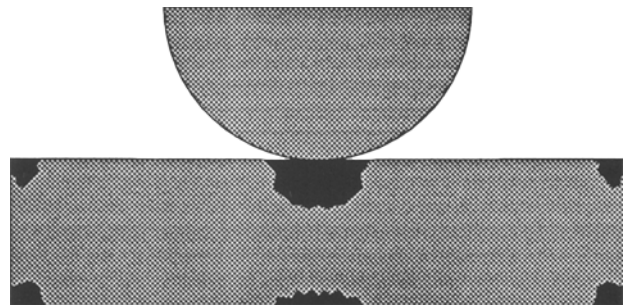


Fig. 7. Second mesh, plastic zone,  $t = 2.5$

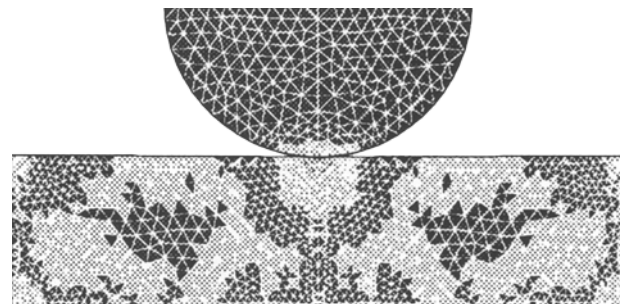


Fig. 8. Second mesh, error distribution

Refinement occurs at time  $t = 1.5$ ,  $t = 2.5$  and  $t = 3.0$ . At these times the plastic zone is depicted before and after mesh refinement. Additionally, the plastic zone for the time  $t = 3.5$  is shown. Plastic regions are denoted by darkgrey and elastic regions are plotted in lightgrey color. Elements, which error values violate (48), are indicated in Figs. 4, 8 and 12

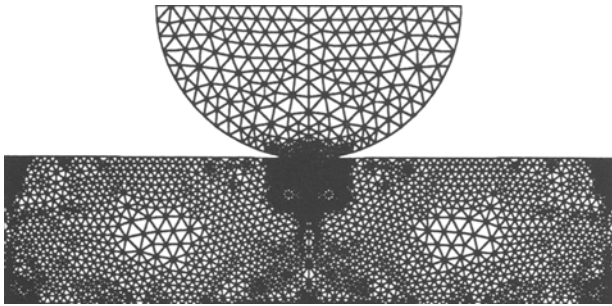


Fig. 9. Third mesh, 1416 nodes, 2640 elements

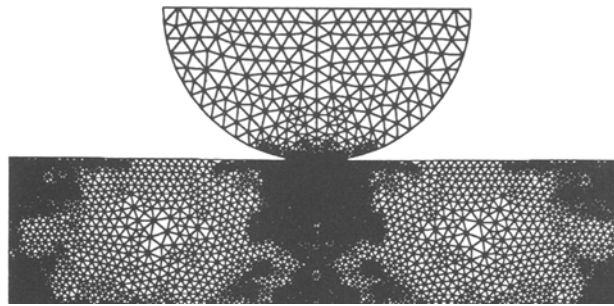


Fig. 13. Final mesh, 2785 nodes, 5299 elements

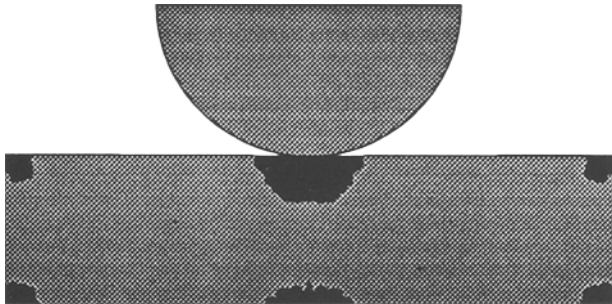


Fig. 10. Third mesh, plastic zone,  $t = 2.5$

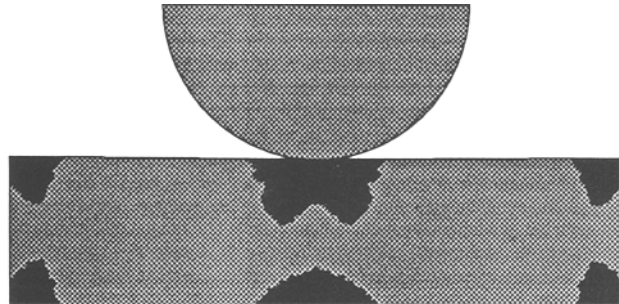


Fig. 14. Final mesh, plastic zone,  $t = 3.0$

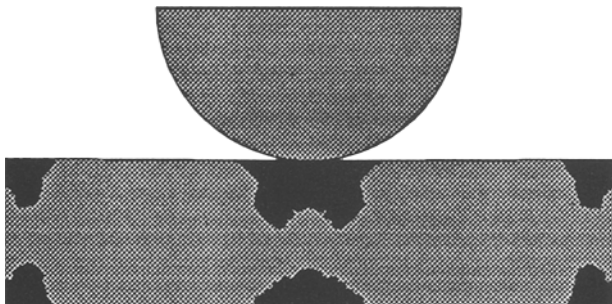


Fig. 11. Third mesh, plastic zone,  $t = 3.0$

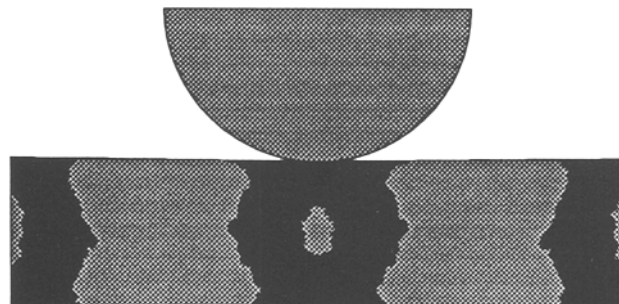


Fig. 15. Final mesh, plastic zone,  $t = 3.5$

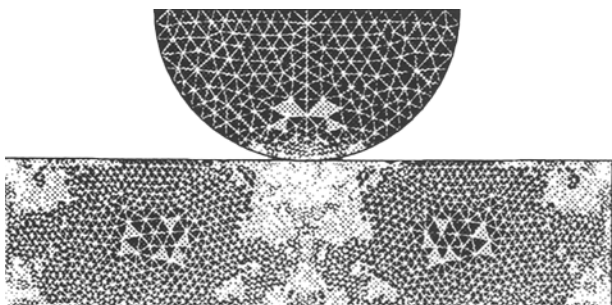


Fig. 12. Third mesh, error distribution

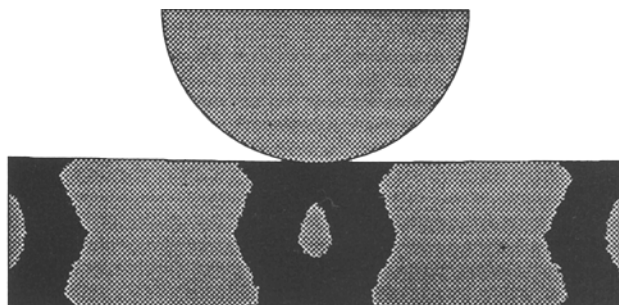


Fig. 16. Reference mesh, plastic zone,  $t = 3.5$

lightgrey, whereas elements, which are not refined, are represented darkgrey. We observe that the error occurs mainly in the plastic region and in the contact interface.

Since the FE-solution of elastoplastic problems depends on the history, an inaccurate approximation of the history variables is attended with irreversible negative effects

concerning the results of the succeeding time steps. Therefore we compare the solution of our adaptive computations with the results obtained by using a uniformly refined reference mesh with 7721 nodes and 14960 elements. The associated picture of the plastic zone at time  $t = 3.5$  is given in Fig. 16, which compares well with Fig. 15 of the adaptive method.



The distribution of the normal stress in 1-direction  $\sigma_{11}$  (see Fig. 2 for the associated coordinate system) is shown for the adapted mesh at time  $t = 3.5$  in Fig. 17. Figure 18 reports the  $\sigma_{11}$ -distribution for the reference mesh. The same scale is used for the isolines in both stress plots. Only very small deviations can be observed.

Finally, we compare in Table 1 the displacements at several points in the structure obtained by the refined mesh and the reference mesh at time  $t = 3.5$ . In addition, we give for point 1 the displacement computed with 4-node quadrilateral elements in an enhanced formulation, see Simo and Rifai [19], at  $t = 3.5$ . This type of element has the advantage to show no locking effects in the case of bending problems and

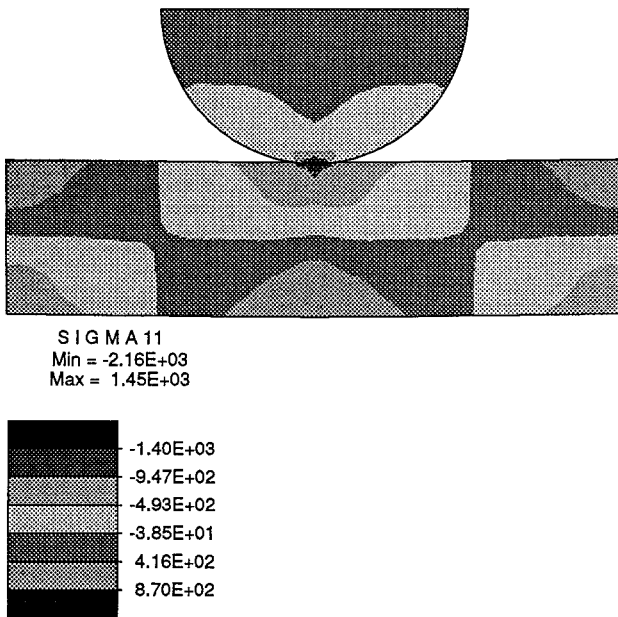


Fig. 17. Adaptive computation,  $\sigma_{11}$ ,  $t = 3.5$

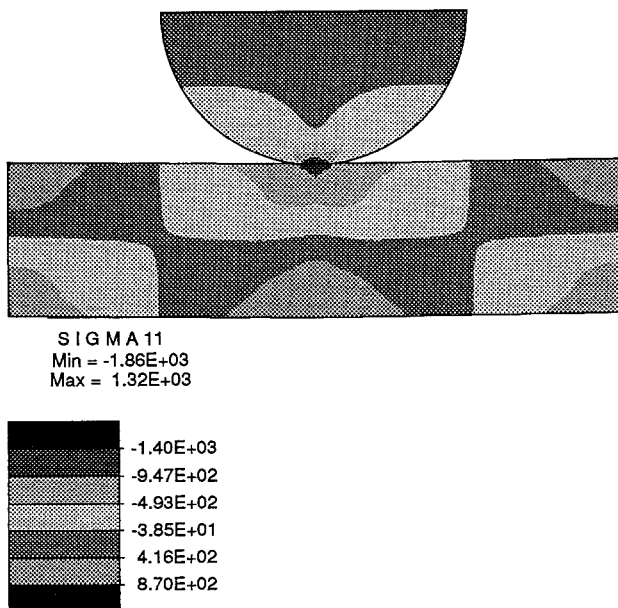


Fig. 18. Reference mesh,  $\sigma_{11}$ ,  $t = 3.5$

Table 1. Displacements,  $t = 3.5$

| Point | 1-displacement         | 2-displacement         |                         |
|-------|------------------------|------------------------|-------------------------|
| 1     | 0                      | $-1.841 \cdot 10^{-2}$ | Refined mesh            |
| 1     | 0                      | $-1.886 \cdot 10^{-2}$ | Reference mesh          |
| 1     | 0                      | $-1.856 \cdot 10^{-2}$ | Enhanced $40 \times 20$ |
| 2     | 0                      | $-2.640 \cdot 10^{-2}$ | Refined mesh            |
| 2     | 0                      | $-2.673 \cdot 10^{-2}$ | Reference mesh          |
| 3     | $-3.267 \cdot 10^{-3}$ | $-1.698 \cdot 10^{-2}$ | Refined mesh            |
| 3     | $-3.338 \cdot 10^{-3}$ | $-1.737 \cdot 10^{-2}$ | Reference mesh          |

incompressibility constraints. We discretise only half of the beam and use a mesh with 40 elements in 1-direction and 20 elements in 2-direction. In this mesh the load is applied as a single load at the center of the upper side of the beam. The coordinates of point 1 are  $(0, -2)$ , of point 2  $(0, -1)$  and of point 3  $(0.4, -1)$ . The associated coordinate system is shown in Fig. 2. As for the stresses, only small deviations are observed. The differences between reference and adaptive solution stem from the finer resolution of the reference mesh in the elastic zone.

## References

- Babuska, I.; Miller, A. 1987: A feedback finite element method with a posteriori error estimation: Part I. The finite element method and some basic properties of the a posteriori error estimation, *Comp. Meth. Appl. Mech. Engrg.*, 61: 1–40
- Babuska, I.; Rheinboldt, W. 1978: Error estimates for adaptive finite element computations, *J. Num. Analysis*, 15: 736–754
- Carstensen, C.; Scherf, O.; Wriggers, P.: A posteriori estimate and adaptive mesh refinement for contact of elastic bodies, submitted to *Comp. Meth. Appl. Mech. Engrg.*
- Hlavacek, I.; Haslinger, J.; Necas, J.; Lovisek, J. 1988: *Solution of Variational Inequalities in Mechanics*, Springer, New York
- Johnson, C. 1987: *Numerical Solutions of Partial Differential Equations by the Finite Element Method*, Cambridge Press, New York
- Johnson, C. 1991: Adaptive finite element methods for the obstacle problem, Technical Report, Chalmers University of Technology, Göteborg
- Johnson, C.; Hansbo, P. 1992: Adaptive finite element methods in computational mechanics, *Comp. Meth. Appl. Mech. Engrg.*, 101: 143–181
- Kikuchi, N.; Oden, J. T. 1988: *Contact Problems in Elasticity: A Study of Variational Inequalities and Finite Element Methods*, SIAM, Philadelphia
- Krieg, R. D.; Krieg, D. B. 1977: Accuracies of numerical Solution Methods for the elastic–perfectly plastic model, *J. Press. Vessel Techn.*, ASME, 99
- Laursen, T. A.; Simo, J. C. 1991: On the the formulation and numerical treatment of finite deformation frictional contact problems, in: *Computational Methods in Nonlinear Mechanics*, P. Wriggers, W. Wagner, eds., Springer, Berlin
- Lee, C. Y.; Oden, J. T.; Ainsworth, M. 1991: Local a posteriori error estimates and numerical results for contact problems and problems of flow through porous media, in: *Nonlinear Computational Mechanics* P. Wriggers, P. Wagner, eds., 671–689, Springer, Berlin
- Luenberger, D. G. 1984: *Linear and nonlinear programming*, Addison Wesley, Reading
- Ortiz, M.; Popov, E. P. 1985: Accuracy and stability of integration algorithms for elastoplastic constitutive equation, *Int. J. Num. Meth. Engrg.*, 21: 1561–1576
- Ortiz, M.; Quigley IV, J. J. 1991: Adaptive mesh refinement in strain localization problems, *Comp. Meth. Appl. Mech. Engrg.*, 90: 781–804

- Peraire, J.; Vahdati, M.; Morgan, K. Zienkiewicz, O. C.** 1987: Adaptive meshing for compressible flow computations, *J. Comp. Phys.*, 72: 449–466
- Peric, D.; Yu, J.; Owen, D. R. J.** 1994: On error estimates and adaptivity in elastoplastic solid: Applications to the numerical simulation of strain localization in classical and Cosserat continua, *Int. J. Num. Meth. Engrg.*, 37: 1351–1379
- Simo, J. C.** 1991: Nonlinear stability of the time discrete variational problem in nonlinear heat conduction and elastoplasticity, *Comp. Meth. Appl. Mech. Engrg.*, 88: 111–121
- Simo, J. C.** 1995: Topics on the numerical analysis and simulation of plasticity, *Handbook of Numerical Analysis*, Vol III, P. G. Ciarlet, J. L. Lions, eds., Elsevier
- Simo, J. C.; Rifai, M. S.** 1990: A class of mixed assumed strain methods and the method of incompatible modes, *Int. J. Num. Meth. Engrg.*, 29: 1595–1638
- Simo, J. C.; Taylor, R. L.** 1985: Consistent tangent operators for rate-independent elastoplasticity, *Comp. Meth. Appl. Mech. Engrg.*, 48: 101–118
- Sloan, S. W.** 1987: A fast algorithm for constructing delaunay triangularization in the plane, *Adv. Eng. Software*, 9: 34–55
- Wriggers, P.; Miehe, C.** 1994: Contact constraints within coupled thermomechanical analysis – A finite element model, *Comp. Meth. Appl. Mech. Engrg.*, 113: 301–319
- Wriggers, P.; Scherf, O.; Carstensen, C.** 1994: Adaptive techniques for the contact of elastic bodies, in: *Recent Developments in Finite Element Analysis*, T. J. R. Hughes, E. Onate, O. C. Zienkiewicz, eds., CIMNE, Barcelona
- Zienkiewicz, O. C.; Liu, Y. C.; Huang, G. C.** 1988: Error estimation and adaptivity in flow formulation for forming problems, *Int. J. Num. Meth. Engrg.*, 25: 23–42
- Zienkiewicz, O. C.; Taylor R. L.** 1988: *The finite element method*, 4th ed., Vol. I, McGraw Hill, London
- Zienkiewicz, O. C.; Zhu, J. Z.** 1987: A simple error estimator and adaptive procedure for practical engineering analysis, *Int. J. Num. Meth. Engrg.*, 24: 337–357
- Zienkiewicz, O. C.; Zhu, J. Z.** 1992: The superconvergent patch recovery and a posteriori error estimates. Part 1: The recovery technique. *Int. J. Num. Meth. Engrg.*, 33: 1331–1364